Husimi function and phase-space analysis of bilayer quantum Hall systems at $\nu = 2/\lambda$

M. Calixto and C. Peón-Nieto

Departamento de Matemática Aplicada and Instituto "Carlos I" de Física Teórica y Computacional,
Universidad de Granada, Fuentenueva s/n, 18071 Granada, Spain

(Dated: September 11, 2021)

We propose localization measures in phase space of the ground state of bilayer quantum Hall (BLQH) systems at fractional filling factors $\nu = 2/\lambda$, to characterize the three quantum phases (shortly denoted by spin, canted and ppin) for arbitrary $U(4)$-isospin λ. We use a coherent state (Bargmann) representation of quantum states, as holomorphic functions in the 8-dimensional Grassmannian phase-space $\mathbb{G}_2^4 = U(4)/[U(2) \times U(2)]$ (a higher-dimensional generalization of the Haldane's 2-dimensional sphere $\mathbb{S}^2 = U(2)/[U(1) \times U(1)]$). We quantify the localization (inverse volume) of the ground state wave function in phase-space throughout the phase diagram (i.e., as a function of Zeeman, tunneling, layer distance, etc, control parameters) with the Husimi function second moment, a kind of inverse participation ratio that behaves as an order parameter. Then we visualize the different ground state structure in phase space of the three quantum phases, the canted phase displaying a much higher delocalization (a Schrödinger cat structure) than the spin and ppin phases, where the ground state is highly coherent. We find a good agreement between analytic (variational) and numeric diagonalization results.

I. INTRODUCTION

Information theoretic and statistical measures have proved to be useful in the description and characterization of quantum phase transitions (QPTs). For example, in the traditional Anderson metal-insulator transition [1–5], Hamiltonian eigenfunctions underlie strong fluctuations. Also, the localization of the electronic wave function can be regarded as the key manifestation of quantum coherence at a macroscopic scale in a condensed matter system. In this article we want to analyze QPTs in BLQH systems at fractional filling factors $\nu = 2/\lambda$ from an information theoretic perspective. The integer case $\nu = 2$ has been extensively studied in the literature (see e.g. [6–12]), where the analysis of the ground state structure reveals the existence of (in general) three quantum phases, shortly denoted by: spin, canted and ppin [6, 7], depending on which order parameter (spin or pseudospin/layer) dominates across the control parameter space: tunneling, Zeeman, bias voltage, etc, couplings. Here we shall study localization properties in phase-space of the ground state in each of the three quantum phases for arbitrary λ (number of magnetic flux quanta per electron). For it, we shall use a phase-space representation $\langle Z|\psi\rangle = \psi(Z)$ of quantum states $|\psi\rangle$, where $|Z\rangle$ denotes and arbitrary coherent (minimal uncertainty) state labeled by points $Z \in \mathbb{G}_2^4 = U(4)/[U(2) \times U(2)] \simeq \mathrm{Mat}_{2\times 2}(\mathbb{C})$ (2×2 complex matrices), the complex Grassmannian with complex dimension 4. The Grassmannian $\mathbb{G}_2^4$ can be seen as a higher-dimensional generalization of the Haldane's sphere $\mathbb{S}^2 = U(2)/[U(1) \times U(1)]$ [13] for monolayer fractional QH systems, with Z a 2×2 matrix generalization of the stereographic projection $z = \tan(\theta/2)e^{i\phi}$ of a point (θ, ϕ) (polar and azimuthal angles) of the Riemann sphere $\mathbb{S}^2$ onto the complex plane. Standard spin-s coherent states (CS) on the sphere $\mathbb{S}^2 = \mathbb{C}P^1$ (iso-

morphic to the complex projective space) are very well known (see traditional references [14–17] on CS and later on section II). Its extension to the complex projective space $\mathbb{C}P^{N-1} = U(N)/[U(N-1) \times U(1)]$ (the symmetric case) is quite straightforward and $\mathbb{C}P^{N-1}$ is related to the phase space of N-component QH systems at fractional values of $\nu = 1$. The case $1 < \nu < N/2+1$ is much more involved and the phase space is the complex Grassmannian $\mathbb{G}_M^N = U(N)/[U(M) \times U(N-M)]$ for fractional values of $\nu = M$. The 4-component (spin-layer) CS on $\mathbb{G}_2^4$ for fractional values $\nu = 2/\lambda$ of $\nu = 2$ have been introduced in [18–20] and recently extended to the N-component case $\mathbb{G}_M^N$ for filling factors $\nu = M/\lambda$ in [21]. In [22] we have used these CS as variational states to study the classical limit and phase diagram of BLQH systems at $\nu = 2/\lambda$. Here we are interested in the CS (phase-space or Bargmann) representation $\langle Z|\psi\rangle = \psi(Z)$ of quantum states $|\psi\rangle$, the squared norm $Q_\psi(Z) = |\psi(Z)|^2$ being a positive quasi-probability distribution called the Husimi or Q-function. Both, Husimi and Wigner, phase-space quasi-probability distributions are useful to characterize phase-space properties of many quantum systems, specially in Quantum Optics [23], although Husimi proves sometimes to be more convenient because, unlike Wigner, it is non-negative. It can also be measured by tomographic, spectroscopic, interferometric, etc, techniques, allowing a quantum state reconstruction. For example, one can visualize the time evolution of CS of light in a Kerr medium by measuring Q_ψ by cavity state tomography [24]. Moreover, the zeros of the Husimi function have been used as an indicator of the regular or chaotic behavior in quantum maps for a variety of atomic, molecular [25, 26], condensed matter systems [27], etc. Information theoretic measures of Q_ψ have also been considered as an indicator of metal-insulator [4] and topological-band insulator [28] phase transitions, together with other

QPTs in Dicke, vibron, Lipkin-Meshkov-Glick (LMG), BEC and Bardeen-Cooper-Schrieffer (BCS) models [29–34], etc. In this article, we shall explore this phase-space tool to extract semi-classical information from the ground state of BLQH systems.

Using a CS representation, we shall obtain the Husimi function $Q_\psi(Z)$ of the ground state ψ of a BLQH system at $\nu = 2/\lambda$. This representation will allow us to visualize the structure of the ground state ψ in phase-space in each of the three quantum phases (spin, canted and ppin). The Hamiltonian we shall use is an adaptation of the integer $\nu = 2$ case [6] to the fractional $\nu = 2/\lambda$ case [22]. The localization of ψ in phase-space can be quantified by the Husimi function second moment $M_\psi = \int_{\mathbb{G}_2^4} Q_\psi^2(Z) d\mu(Z)$, where $d\mu(Z)$ denotes a proper measure on $\mathbb{G}_2^4$ (see later). Maximal localization (minimum volume/uncertainty) in phase space is attained when ψ is itself a CS. This statement is in fact a conjecture that was proved for harmonic oscillator CS [35] and recently for the particular case of $SU(2)$ spin-s CS [36]. Here we check the validity of this conjecture for Grassmannian $\mathbb{G}_2^4$ CS. In fact, we obtain that the ground state in spin and ppin phases is highly coherent (maximally localized), whereas it is more delocalized (higher uncertainty) in the canted phase, having the structure of a "Schrödinger cat", that is, a quantum superposition of two semi-classical states with negligible overlap [see later on eq. (43)].

The organization of the paper is as follows. In section II we use the Haldane sphere picture for the (simpler) monolayer case to introduce some basic concepts like "creation and annihilation operators of magnetic flux quanta" and the coherent state (Bargmann-Fock) representation of quantum states, which will be essential to analyze the structure, semi-classical and localization properties of the ground state. In section III we extend the spin-s $U(2)$ symmetry to the isospin-λ $U(4)$ symmetry, providing an oscillator realization of the $U(4)$ operators and the Landau-site Hilbert space for $\nu = 2/\lambda$. We also review the isospin-λ coherent states on $\mathbb{G}_2^4$, which are essential for the semiclassical ground state analysis of BLQH systems discussed in subsequent sections and to introduce the Husimi function and localization measures in phase space. Most of the construction has been already discussed in references [18–20]; here we give a brief for the sake of self-containedness. In section IV we study the Landau-site Hamiltonian governing the BLQH system at $\nu = 2/\lambda$, which is an adaptation of the one proposed in [6] for $\lambda = 1$ to the fractional case (arbitrary odd λ); this Hamiltonian has already been discussed in [22]. Using CS expectation values of the Hamiltonian, we perform a semiclassical analysis and a study of its quantum phases. In section V we make a variational and exact (numerical diagonalization) ground state analysis and characterize the quantum phases (spin, ppin and canted) using localization measures in phase space. Variational results agree with numerical diagonalization calculations and provide analytical formulas for some physical quantities. The last section is left for conclusions and outlook.

II. HALDANE SPHERE U(2) PICTURE

Firstly, we shall rephrase the simpler monolayer case in order to introduce the basic ingredients of the CS or Bargman picture. The technical innovation of Haldane [13] was to place the 2D electron gas on a spherical surface in a radial (monopole) magnetic field. Then, the total magnetic flux through the surface is an integer $2s$ times the flux quantum $\Phi_0 = h/e$, as required by Dirac's monopole quantization. The Hilbert space of the lowest Landau level is spanned by polynomials in the spinor coordinates $u = \cos(\theta/2) \exp(i\phi/2)$ and $v = \sin(\theta/2) \exp(-i\phi/2)$ of total degree $2s$ (θ, ϕ denote the polar and azimuthal angles on the sphere, respectively). Within this subspace, the electron may be represented by a spin s, the orientation of which indicates the point (θ, ϕ) of the sphere about which the state is localized. Multiplication by u and v may also be represented as independent boson creation operators $a_\uparrow^\dagger$ and $a_\downarrow^\dagger$ of magnetic flux quanta (flux quanta in the sequel) attached to the spin-up and spin-down electron respectively. In the same way, derivation by ∂/∂_u and ∂/∂_v may also be represented as independent boson annihilation operators $a_\uparrow$ and $a_\downarrow$ of flux quanta attached to the electron. This is related to the composite fermion picture [37] of fractional QH effect, according to wich, bosonic flux quanta are attached to the electrons to form composite fermions. The spin density operator $\vec{S}$ can be written in terms of these creation and annihilation operators of flux quanta as (the Jordan-Schwinger boson realization for spin)

$$S_+ = a_\uparrow^\dagger a_\downarrow, \ S_- = a_\downarrow^\dagger a_\uparrow, \ S_3 = (a_\uparrow^\dagger a_\uparrow - a_\downarrow^\dagger a_\downarrow)/2. \quad (1)$$

This expression can be compactly written as

$$S_\mu = \frac{1}{2}\zeta^\dagger \sigma_\mu \zeta, \ \mu = 0, 1, 2, 3, \quad (2)$$

in terms of the two-component electron "field" $\zeta = \begin{pmatrix} a_\uparrow \\ a_\downarrow \end{pmatrix}$ and its conjugate $\zeta^\dagger = (a_\uparrow^\dagger, a_\downarrow^\dagger)$, where $\sigma_\mu, \mu = 1, 2, 3$, denote the usual three Pauli matrices plus σ_0 (the 2×2 identity matrix). The four operators S_μ close the Lie algebra of $U(2)$. Actually, the extra operator $2S_0 = \zeta^\dagger \zeta = a_\uparrow^\dagger a_\uparrow + a_\downarrow^\dagger a_\downarrow$ represents the total number $n_\uparrow + n_\downarrow = 2s$ (twice the spin s) of flux quanta, which is conserved since $[S_0, \vec{S}] = 0$. The spin third component S_3 measures the flux quanta imbalance between spin up and down, whereas $S_\pm = S_1 \pm iS_2$ are tunneling (ladder) operators that transfer flux quanta from spin up to down and vice versa, creating spin coherence.

The boson realization (2) defines a unitary representation of the spin $U(2)$ operators S_μ on the Fock space expanded by the orthonormal basis states

$$|n_\uparrow\rangle \otimes |n_\downarrow\rangle = \frac{(a_\uparrow^\dagger)^{n_\uparrow}(a_\downarrow^\dagger)^{n_\downarrow}}{\sqrt{n_\uparrow! n_\downarrow!}} |0\rangle_{\mathrm{F}}, \quad (3)$$

where $|0\rangle_F$ denotes the Fock vacuum and $n_{\uparrow(\downarrow)}$ the number of flux quanta attached to spin up (down). The fact that $2S_0$ is conserved indicates that the representation (2) is reducible in Fock space. A $(2s+1)$-dimensional irreducible (Hilbert) subspace $\mathcal{H}_s(\mathbb{S}^2)$ carrying a unitary representation of $U(2)$ with spin s is expanded by the S_3 eigenvectors

$$|k\rangle \equiv |s+k\rangle_\uparrow \otimes |s-k\rangle_\downarrow = \frac{\varphi_k(a_\uparrow^\dagger)}{\sqrt{\frac{(2s)!}{(s+k)!}}} \frac{\varphi_{-k}(a_\downarrow^\dagger)}{\sqrt{\frac{(2s)!}{(s-k)!}}}|0\rangle_F, \quad (4)$$

with $k = -s, \ldots, s$ the corresponding spin third component [flux quanta imbalance $(n_\uparrow - n_\downarrow)/2$] and $\varphi_k(z) = \binom{2s}{s+k}^{1/2} z^{s+k}$. We have made use of the monomials $\varphi_k(z)$ as a useful notation to generalize the Fock space representation (4) of the spin-s $U(2)$ states $|k\rangle$, to the isospin-λ $U(4)$ states $|_{q_a,q_b}^{j,m}\rangle$ in eq. (17). The monomials $\varphi_k(z)$ verify the closure relation

$$\sum_{k=-s}^{2} \overline{\varphi_k(z')}\varphi_k(z) = K_s(\bar{z}', z), \quad (5)$$

with $K_s(\bar{z}', z) = (1 + \bar{z}'z)^{2s}$ the so-called Bergmann kernel for spin-s [see (20) for its generalization to the bilayer case $U(4)$]. $\mathcal{H}_s(\mathbb{S}^2)$ is then the carrier space of the $(2s+1)$-dimensional totally symmetric unitary irreducible representation that arises in the Clebsch-Gordan decomposition of a tensor product of $2s$ two-dimensional (fundamental, elementary) representations of $U(2)$; for example, in Young tableau notation:

$$\overbrace{\square \otimes \cdots \otimes \square}^{2s} = \overbrace{\boxed{\boxed{\cdots}}}^{2s} \oplus \ldots, \quad (6)$$

or $\overbrace{[1] \otimes \cdots \otimes [1]}^{2s} = [2s] \oplus \ldots$. This Young tableau notation will be usefull when interpreting the bilayer case at fractional values of $\nu = 2$ in a group theoretical context [see expression (15)].

As already said, the operators $S_\pm$ create spin coherence, which can be described by spin-s CS

$$|z\rangle = \frac{e^{zS_+}|-s\rangle}{(1+|z|^2)^s} = \frac{\sum_{k=-s}^{s} \varphi_k(z)|k\rangle}{(1+|z|^2)^s}, \quad (7)$$

obtained as an exponential action of the rising operator S_+ on the lowest-weight state $|k = -s\rangle$ (namely, all flux quanta attached to spin down electron). The coherence strength $z = v/u = \tan(\theta/2)e^{-i\phi}$ is the quotient of the spinor coordinates u and v defined above and is related to the stereographic projection of a point (θ, ϕ) of the sphere $\mathbb{S}^2 = U(2)/U(1)^2$ onto the complex plane. In other words, the CS $|z\rangle$ is the rotation of the state $|k = -s\rangle$ about the axis $\vec{r} = (\sin\phi, -\cos\phi, 0)$ in the $x - y$ plane by an angle θ. Perhaps, a more familiar Fock-space representation of spin-s CS [equivalent to (7)] is given as

a two-mode Bose-Einstein condensate

$$|z\rangle = \frac{1}{\sqrt{(2s)!}} \left(\frac{a_\downarrow^\dagger + za_\uparrow^\dagger}{\sqrt{1+|z|^2}} \right)^{2s} |0\rangle_F. \quad (8)$$

In this context, the polar angle θ is related to the population imbalance $s\cos\theta$ (the spin third component expectation value $\langle z|S_3|z\rangle$) between modes and the azimuthal angle ϕ is the relative phase (coherence). Both quantities can be experimentally determined in terms of matter-wave interference experiments (see e.g.[38]).

From the mathematical point of view, spin-s CS are normalized (but not orthogonal), as can be seen from the CS overlap

$$\langle z'|z\rangle = K_s(\bar{z}', z)/[K_{s/2}(\bar{z}', z')K_{s/2}(\bar{z}, z)], \quad (9)$$

written in terms of the Bergmann kernel (5). CS constitute an overcomplete set fulfilling the resolution of the identity $1 = \int_{\mathbb{S}^2} |z\rangle\langle z|d\mu(z, \bar{z})$, with $d\mu(z, \bar{z}) = \frac{2s+1}{\pi}\sin\theta d\theta d\phi$ the solid angle.

Spin-s CS have minimal uncertainty and therefore they are suitable to study the semi-classical, mean-field or thermodynamical limit of many spin systems, specially those undergoing a QPT. The semi-classical properties of a quantum spin state $|\psi\rangle$ are better described in a CS or Fock-Bargmann representation of any spin state $\psi \in \mathcal{H}_s(\mathbb{S}^2)$ defined as $\Psi(z) = K_{s/2}(\bar{z}, z)\langle\psi|z\rangle$. For example, the basis states $|\psi\rangle = |k\rangle$ are represented by the monomials $\varphi_k(z) = \binom{2s}{s+k}^{1/2} z^{s+k}$ in (4), whereas a general spin state $|\psi\rangle = \sum_{k=-s}^{s} c_k|k\rangle$ is represented by a polynomial $\Psi(z) = \sum_{k=-s}^{s} \bar{c}_k\varphi_k(z)$ of degree $2s$ in z. Inside this CS picture, spin operators (1) are represented by differential operators

$$\mathcal{S}_+ = -z^2\frac{d}{dz} + 2sz, \ \mathcal{S}_- = \frac{d}{dz}, \ \mathcal{S}_3 = z\frac{d}{dz} - s, \quad (10)$$

so that the following the identity $\mathcal{S}_i\Psi(z) = K_{s/2}(\bar{z}, z)\langle\psi|S_i|z\rangle$ holds. In other words, $\mathcal{S}_i$ are the infinitesimal generators of Möbius transformations $z' = (az + b)/(cz + d)$ of z under a $SU(2)$ group translation $U = \begin{pmatrix} a & b \\ c & d \end{pmatrix}$. This differential realization of the $SU(2)$ spin generators is useful for technical calculations like CS expectation values and matrix elements

$$\langle z'|S_i|z\rangle = [K_{s/2}(\bar{z}, z)K_{s/2}(\bar{z}', z')]^{-1}\mathcal{S}_iK_s(\bar{z}', z), \quad (11)$$

which are reduced to simple derivatives of the Bergmann kernel. For example $\langle z|S_3|z\rangle = s(|z|^2 - 1)/(|z|^2 + 1) = -s\cos\theta$. We shall make extensive use of this relation when computing the energy surface (the CS Hamiltonian expectation value).

The probability density in this CS representation is the so-called Husimi quasiprobability distribution function $Q_\psi(z) = |\langle z|\psi\rangle|^2$. Basically, $Q_\psi(z)$ is the probability to measure the spin third component $k = -s$ (all flux quanta attached to spin down electron) in ψ

in an orientation given by (θ, ϕ). For a general spin state $|\psi\rangle = \sum_{k=-s}^{s} c_k |k\rangle$, the Husimi amplitude $\langle \psi | z \rangle$ is basically a polynomial in z (except for a normalization factor) of degree $2s$, which can be determined by a finite number of measurements, thus allowing a state reconstruction.

For normalized states $\langle \psi | \psi \rangle$, the resolution of the identity $1 = \int_{\mathbb{S}^2} |z\rangle \langle z| d\mu(z, \bar{z})$ indicates that the quasiprobability distribution Q_ψ is normalized $\int_{\mathbb{S}^2} Q_\psi(z) d\mu(z, \bar{z}) = 1$. The Husimi second moment

$$M_\psi = \int_{\mathbb{S}^2} Q_\psi^2(z) d\mu(z, \bar{z}), \qquad (12)$$

also called "inverse participation ratio" (IPR), will be an important quantity for us. Broadly speaking, the IPR measures the spread of a state $|\psi\rangle$ over a basis $\{|i\rangle\}_{i=1}^d$. Precisely, if p_i is the probability of finding the (normalized) state $|\psi\rangle$ in $|i\rangle$, then the IPR is defined as $M_\psi = \sum_i p_i^2$. If $|\psi\rangle$ only "participates" of a single state $|i_0\rangle$, then $p_{i_0} = 1$ and $M_\psi = 1$ (large IPR), whereas if $|\psi\rangle$ equally participates on all of them (equally distributed), $p_i = 1/d, \forall i$, then $M_\psi = 1/d$ (small IPR). Therefore, the IPR is a measure of the localization of $|\psi\rangle$ in the corresponding basis. For our case, the Husimi second moment (12) measures how close is $|\psi\rangle$ to a coherent state $|Z\rangle$. M_ψ attains its maximum value $M_{\max} = 1/2 + 1/(2 + 8s)$ (maximum localization) when $|\psi\rangle$ is itself a (minimum uncertainty) CS (see [36] for a proof). There are other localization measures of ψ, quantifying the area occupied by Q_ψ in the sphere $\mathbb{S}^2$, like the Wehrl entropy $W_\psi = \int_{\mathbb{S}^2} Q_\psi(z) \ln Q_\psi(z) d\mu(z, \bar{z})$, but we shall use M_ψ because it is easier to compute and provides similar qualitative information.

Localization measures defined in terms of the Husimi function have proved to be a good tool to analize QPTs in Hamiltonian systems written in terms of $SU(2)$ collective generators $\vec{S}$ like, for example, Dicke, vibron, LMG, BEC and BCS models [29–34], etc. The Husimi function Q_ψ provides essential information and, in particular, its zeros, which turn out to be related to pairing energies in LMG and BCS pairing mean-field Hamiltonians. In the next sections, we use the Husimi function to extract information about the quantum phases that appear in BLQH systems at $\nu = 2/\lambda$ for Hamiltonians written in terms of $U(4)$ collective operators $\vec{S}, \vec{P}$ and $\mathbf{R}$.

III. GRASSMANNIAN U(4) PICTURE FOR THE BILAYER CASE

A. U(4) symmetry and bosonic flux quanta representation

The bilayer case introduces a new degree of freedom (layer or pseudospin) to the electron and, therefore, BLQH systems underlie an isospin $U(4)$ symmetry. Inside the composite fermion picture exposed in the previous section, bosonic magnetic flux quanta are attached to the electrons to form composite fermions in the fractional case. Let us denote by $(a_l^\downarrow)^\dagger$ [resp. $(b_l^\uparrow)^\dagger$] creation operators of flux quanta attached to the electron l with spin down [resp. up] at layer a [resp. b], and so on. For the case of filling factor $\nu = 2$ (two electrons, $l = 1, 2$, per Landau site) the electron "field" ζ is now arranged as a four-component compound $\zeta = (\zeta_1, \zeta_2)$ of two fermions. The sixteen $U(4)$ density operators are then written as bilinear products of creation and annihilation operators as [remember the expression (2) for $U(2)$ spin operators]

$$T_{\mu\nu} = \text{tr}(\zeta^\dagger \tau_{\mu\nu} \zeta), \quad \zeta = \begin{pmatrix} \mathbf{a} \\ \mathbf{b} \end{pmatrix} = \begin{pmatrix} a_1^\downarrow & a_2^\downarrow \\ a_1^\uparrow & a_2^\uparrow \\ b_1^\uparrow & b_2^\uparrow \\ b_1^\downarrow & b_2^\downarrow \end{pmatrix}, \qquad (13)$$

where the sixteen 4×4 matrices $\tau_{\mu\nu} \equiv \sigma_\mu^{\text{ppin}} \otimes \sigma_\nu^{\text{spin}}$, $\mu, \nu = 0, 1, 2, 3$, denote the $U(4)$ generators in the four-dimensional fundamental representation [they are written as a tensor product of spin and pseudospin/layer (ppin for short) Pauli matrices]. In the BLQH literature (see e.g. [7]) it is customary to denote the total spin $S_k = T_{0k}/2$ and ppin $P_k = T_{k0}/2$, together with the remaining 9 isospin $R_{kl} = T_{lk}/2$ operators for $k, l = 1, 2, 3$. A constraint in the Fock space of eight boson modes is imposed such that $\zeta^\dagger \zeta = \lambda I_2$, with λ representing the number of flux quanta bound to each electron and I_2 the 2×2 identity. In particular, the linear Casimir operator $T_{00} = \text{tr}(\zeta^\dagger \zeta)$, providing the total number of flux quanta, is fixed to $n_a + n_b = \lambda + \lambda = 2\lambda$, with $n_a = n_{a1}^\uparrow + n_{a1}^\downarrow + n_{a2}^\uparrow + n_{a2}^\downarrow$ the total number of flux quanta in layer a (resp. in layer b). The quadratic Casimir operator is also fixed to

$$\vec{S}^2 + \vec{P}^2 + \mathbf{R}^2 = \lambda(\lambda + 4). \qquad (14)$$

We also identify the interlayer imbalance operator P_3 (ppin third component), which measures the excess of flux quanta between layers a and b, that is $\frac{1}{2}(n_a - n_b)$. Therefore, the realization (13) defines a unitary bosonic representation of the $U(4)$ matrix generators $\tau_{\mu\nu}$ in the Fock space of eight modes with constrains. The corresponding Hilbert space will be denoted by $\mathcal{H}_\lambda(\mathbb{G}_2^4)$, which generalizes $\mathcal{H}_s(\mathbb{S}^2)$ for the monolayer case. The dimension of $\mathcal{H}_\lambda(\mathbb{G}_2^4)$ corresponds to the different ways to attach 2λ flux quanta to two identical electrons in two layers. The count of states is as follows. The first electron can occupy any of the four isospin states $|b\uparrow\rangle, |b\downarrow\rangle, |a\uparrow\rangle$ and $|a\downarrow\rangle$ at one Landau site of the lowest Landau level. Therefore, there are $\binom{4+\lambda-1}{\lambda}$ ways of distributing λ quanta among these four states. Due to the Pauli exclusion principle, there are only three states left for the second electron and $\binom{3+\lambda-1}{\lambda}$ ways of distributing λ flux quanta among these three states. However, some of the previous configurations must be identified since both electrons are indistinguishable and λ pairs of quanta adopt $\binom{2+\lambda-1}{\lambda}$ equivalent configurations. In total,

there are

$$d_\lambda = \frac{\binom{\lambda+3}{\lambda}\binom{\lambda+2}{\lambda}}{\binom{\lambda+1}{\lambda}} = \frac{1}{12}(\lambda+3)(\lambda+2)^2(\lambda+1)$$

ways to distribute 2λ flux quanta among two identical electrons in four states. This is precisely the dimension of the rectangular Young tableau of shapes $[\lambda, \lambda]$ (2 rows of λ boxes each) arising in the Clebsch-Gordan decomposition of a tensor product of 2λ four-dimensional (fundamental, elementary) representations of $U(4)$

or $\overbrace{[1] \otimes \cdots \otimes [1]}^{2\lambda} = [\lambda, \lambda] \oplus \dots$ This rectangular Young tableaux picture also arises in N-component antiferromagnets [39–41]. Note that quantum states associated to Young tableaux $[\lambda, \lambda]$ are antisymmetric (fermionic character) under the interchange of the two electrons (two rows) for λ odd, whereas they are symmetric (bosonic character) for λ even. Therefore, composite fermions require λ odd.

B. Orthonormal basis and coherent states

In Refs. [18, 19] we have worked out an orthonormal basis

$$B_\lambda(\mathbb{G}_2^4) = \left\{ |^{j,m}_{q_a,q_b}\rangle, \begin{array}{c} 2j, m \in \mathbb{N}, \\ q_a, q_b = -j, \dots, j \end{array} \right\}_{2j+m \leq \lambda}, \quad (16)$$

of the d_λ-dimensional carrier Hilbert space $\mathcal{H}_\lambda(\mathbb{G}_2^4)$, generalizing the spin S_3 eigenvectors $B_s(\mathbb{S}^2) = \{|k\rangle, k = -s, \dots, s\}$ in eq. (4). The orthonormal basis vectors $|^{j,m}_{q_a,q_b}\rangle$ are now indexed by four (half-)integer numbers subject to constraints. We shall provide here a brief summary with the basic expressions, in order to make the article more self-contained (more information can be found in references [18–22]).

Similar to (4) for spin-s states $|k\rangle$, the general expression of these basis states $|^{j,m}_{q_a,q_b}\rangle$ can be given by the action of creation operators $\mathbf{a}^\dagger$ and $\mathbf{b}^\dagger$ of flux quanta on the Fock vacuum $|0\rangle_\text{F}$ as

$$|^{j,m}_{q_a,q_b}\rangle = \frac{1}{\sqrt{2j+1}} \sum_{q=-j}^{j} (-1)^{q_a-q} \quad (17)$$

$$\times \frac{\varphi^{j,m}_{-q,-q_a}(\mathbf{a}^\dagger)}{\sqrt{\frac{\lambda!(\lambda+1)!}{(\lambda-2j-m)!(\lambda+1-m)!}}} \frac{\varphi^{j,\lambda-2j-m}_{q,q_b}(\mathbf{b}^\dagger)}{\sqrt{\frac{\lambda!(\lambda+1)!}{m!(2j+m+1)!}}} |0\rangle_\text{F},$$

where

$$\varphi^{j,m}_{q_a,q_b}(Z) = \sqrt{\frac{2j+1}{\lambda+1}\binom{\lambda+1}{2j+m+1}\binom{\lambda+1}{m}} \quad (18)$$

$$\times \det(Z)^m \mathcal{D}^j_{q_a,q_b}(Z), \begin{array}{c} 2j+m \leq \lambda, \\ q_a, q_b = -j, \dots, j, \end{array}$$

are homogeneous polynomials of degree $2j + 2m$ in four complex variables $z_{uv} \in \mathbb{C}$ arranged in a 2×2 complex matrix $Z = \begin{pmatrix} z_{11} & z_{12} \\ z_{21} & z_{22} \end{pmatrix}$ (a point on the Grassmannian $\mathbb{G}_2^4$). They generalize the monomials $\varphi_k(z) = \binom{2s}{s+k}^{1/2} z^{s+k}$ in (4) for a point z on the sphere $\mathbb{S}^2$. By $\mathcal{D}^j_{q_a,q_b}(Z)$ we denote the usual Wigner $\mathcal{D}$-matrix [42] with angular momentum j. They are homogeneous polynomials of degree $2j$ explicitly given by

$$\mathcal{D}^j_{q_a,q_b}(Z) = \sqrt{\frac{(j+q_a)!(j-q_a)!}{(j+q_b)!(j-q_b)!}} \sum_{k=\max(0,q_a+q_b)}^{\min(j+q_a,j+q_b)} \quad (19)$$

$$\binom{j+q_b}{k}\binom{j-q_b}{k-q_a-q_b} z_{11}^k z_{12}^{j+q_a-k} z_{21}^{j+q_b-k} z_{22}^{k-q_a-q_b}.$$

The closure relation (5) now adopts the following form

$$\sum_{m=0}^{\lambda} \sum_{j=0;\frac{1}{2}}^{(\lambda-m)/2} \sum_{q_a,q_b=-j}^{j} \overline{\varphi^{j,m}_{q_a,q_b}(Z')} \varphi^{j,m}_{q_a,q_b}(Z) = K_\lambda(Z'^\dagger, Z),$$

$$(20)$$

with $K_\lambda(Z'^\dagger, Z) = \det(\sigma_0 + Z'^\dagger Z)^\lambda$ the Bergmann kernel for $\mathbb{G}_2^4$. The orthonormal basis states (17) are eigenstates of the following operators:

$$\begin{aligned} P_3 |^{j,m}_{q_a,q_b}\rangle &= (2j + 2m - \lambda)|^{j,m}_{q_a,q_b}\rangle, \\ (\vec{S}_a^2 + \vec{S}_b^2)|^{j,m}_{q_a,q_b}\rangle &= 2j(j+1)|^{j,m}_{q_a,q_b}\rangle, \quad (21) \\ S_{\ell 3}|^{j,m}_{q_a,q_b}\rangle &= q_\ell |^{j,m}_{q_a,q_b}\rangle, \ \ell = a, b, \end{aligned}$$

where we have defined angular momentum operators in layers a and b as $S_{ak} = -\frac{1}{2}(S_k + R_{k3})$ and $S_{bk} = \frac{1}{2}(S_k - R_{k3})$, $k = 1, 2, 3$, respectively, so that $\vec{S}_a^2 + \vec{S}_b^2 = \frac{1}{2}(\vec{S}^2 + \vec{R}_3^2)$. Therefore, j is a half-integer representing the total angular momentum of layers a and b, whereas q_a and q_b are the corresponding third components. The integer m is related to the interlayer imbalance population (ppin third component P_3) through $\frac{1}{2}(n_a - n_b) = (2j + 2m - \lambda)$; thus, $m = \lambda, j = 0$ means $n_a = 2\lambda$ (i.e., all flux quanta occupying layer a), whereas $m = 0, j = 0$ means $n_b = 2\lambda$ (i.e., all flux quanta occupying layer b). The angular momentum third components q_a, q_b measure the imbalance between spin up and down in each layer, more precisely, $q_a = \frac{1}{2}(n^\uparrow_{a1} - n^\downarrow_{a1} + n^\uparrow_{a2} - n^\downarrow_{a2})$ and similarly for q_b.

Analogously to the two-mode boson (flux quanta) condensate (8), Coherent states on $\mathbb{G}_2^4$ are defined as eight-mode boson condensates (see [18])

$$|Z\rangle = \frac{1}{\lambda!\sqrt{\lambda+1}} \left(\frac{\det(\check{\mathbf{b}}^\dagger + Z^t \check{\mathbf{a}}^\dagger)}{\sqrt{\det(\sigma_0 + Z^\dagger Z)}} \right)^\lambda |0\rangle_\text{F}, \quad (22)$$

where $\check{\mathbf{a}}^\dagger = \frac{1}{2}\eta^{\mu\nu} \text{tr}(\sigma_\mu \mathbf{a}^\dagger)\sigma_\nu$ denotes the "parity reversed" 2×2-matrix creation operator of $\mathbf{a}^\dagger$ in layer a (similar for layer b) [we are using Einstein summation convention with Minkowskian metric $\eta^{\mu\nu} =$

diag$(1, -1, -1, -1)$ for notational convenience]. They can be expanded in the orthonormal basis (16) as

$$|Z\rangle = \frac{\sum_{m=0}^{\lambda} \sum_{j=0;\frac{1}{2}}^{(\lambda-m)/2} \sum_{q_a,q_b=-j}^{j} \varphi_{q_a,q_b}^{j,m}(Z)|_{q_a,q_b}^{j,m}\rangle}{\det(\sigma_0 + Z^\dagger Z)^{\lambda/2}},$$

(23)

with coefficients $\varphi_{q_a,q_b}^{j,m}(Z)$ [compare to (7) for the monolayer case]. Coherent states are normalized, $\langle Z|Z\rangle = 1$, but they do not constitute an orthogonal set since they have a non-zero (in general) overlap given by

$$\langle Z'|Z\rangle = \frac{K_\lambda(Z'^\dagger, Z)}{K_{\lambda/2}(Z'^\dagger, Z')K_{\lambda/2}(Z^\dagger, Z)},$$

(24)

with K_λ the Bergmann kernel in (20).

Using orthogonality properties of the homogeneous polynomials $\varphi_{q_a,q_b}^{j,m}(Z)$, a resolution of unity for isospin-λ CS has been proved in [18], namely $1 = \int_{\mathbb{G}_2^4} |Z\rangle\langle Z| d\mu(Z, Z^\dagger)$, with integration measure [compare with the $\mathbb{S}^2$ measure after (11)]

$$d\mu(Z, Z^\dagger) = \frac{12 d_\lambda}{\pi^4} \frac{\prod_{u,v=1}^{2} d\mathrm{Re}(z_{uv})d\mathrm{Im}(z_{uv})}{\det(\sigma_0 + Z^\dagger Z)^4}.$$

(25)

Instead of the four complex coordinates z_{uv}, we shall use an alternative parametrization of Z in terms of eight angles $\theta_{a,b}, \vartheta_\pm \in [0, \pi)$ and $\phi_{a,b}, \beta_\pm \in [0, 2\pi)$, given by the following decomposition [the analogue of the stereographic projection $z = \tan(\theta/2)e^{i\phi}$ for $\mathbb{S}^2$]

$$Z = V_a \begin{pmatrix} \xi_+ & 0 \\ 0 & \xi_- \end{pmatrix} V_b^\dagger, \ \xi_\pm = \tan\frac{\vartheta_\pm}{2}e^{i\beta_\pm},$$

$$V_\ell = \begin{pmatrix} \cos\frac{\theta_\ell}{2} & -\sin\frac{\theta_\ell}{2}e^{i\phi_\ell} \\ \sin\frac{\theta_\ell}{2}e^{-i\phi_\ell} & \cos\frac{\theta_\ell}{2} \end{pmatrix}, \ \ell = a, b,$$

(26)

where $V_{a,b}$ represent rotations in layers $\ell = a, b$ (note their "conjugated" character). In this coordinate system, the integration measure (25) can be alternatively written as

$$d\mu(Z, Z^\dagger) = \frac{3d_\lambda}{2^9\pi^4}(\cos\vartheta_+ - \cos\vartheta_-)^2 d\Omega_+ d\Omega_- d\Omega_a d\Omega_b,$$

(27)

where $d\Omega_\pm = \sin\vartheta_\pm d\vartheta_\pm d\beta_\pm$ and $d\Omega_\ell = \sin\theta_\ell d\theta_\ell d\phi_\ell$ ($\ell = a, b$) are solid angle elements.

C. Coherent state expectation values and localization in phase space

As commented in section II, for semi-classical considerations is more convenient a CS picture than a Fock space realization of physical states. The Bargmann representation of a general state $|\psi\rangle \in \mathcal{H}_\lambda(\mathbb{G}_2^4)$ given by the overlap $\psi(Z) \equiv \langle Z|\psi\rangle$ between $|\psi\rangle$ and a general CS $|Z\rangle$ like (23). For example, the Bargmann representation of the basis states $|\psi\rangle = |_{q_a,q_b}^{j,m}\rangle$ is given in terms of the homogeneous polynomials in (18) as $\psi(Z) = \varphi_{q_a,q_b}^{j,m}(Z)/K_{\lambda/2}(Z^\dagger, Z)$.

Inside this CS picture, the $U(4)$ isospin generators $\tau_{\mu\nu}$ are represented by differential operators $\mathcal{T}_{\mu\nu}$ [remember (10) for the monolayer case]. They are the infinitesimal generators of Möbius-like transformations on $\mathbb{G}_2^4$

$$Z' = (AZ + B)(CZ + D)^{-1}, \ U = \begin{pmatrix} A & B \\ C & D \end{pmatrix},$$

(28)

under $U \in U(4)$ group translations. For example, it is easy to to see that the differential realization of the imbalance ppin generator $\tau_{k0}/2$ is given by $\mathcal{P}_3 = z^\mu\partial_\mu - \lambda$, where $z^\mu = \mathrm{tr}(Z\sigma_\mu)/2, \mu = 0, 1, 2, 3$. We are using Einstein summation convention and denoting $\partial_\mu = \partial/\partial z^\mu$ and $z_\nu = \eta_{\nu\mu}z^\mu$, with $\eta_{\nu\mu} = \mathrm{diag}(1, -1, -1, -1)$ the Minkowskian metric]. In addition, spin $\mathcal{S}_k$ and $\mathcal{R}_{k3}$ are written in terms of the Lorentz-like generators $\mathcal{M}_{\mu\nu} = z_\mu\partial_\nu - z_\nu\partial_\mu$ as $\mathcal{S}_i = \frac{1}{2}\epsilon^{ikl}\mathcal{M}_{kl}$ and $\mathcal{R}_{k3} = \mathcal{M}_{k0}$, respectively, where ϵ^{ikl} is the totally antisymmetric tensor. The explicit expression of the remainder $U(4)$ differential operators $\mathcal{T}_{\mu\nu}$ can be seen in [18]. Some readers can wonder where this relativistic notation comes from. It is motivated by the fact that $U(4)$ is the compact counterpart of the conformal group $U(2, 2)$, which contains the Poincaré group of special relativity; however, the compacity of $U(4)$ introduces some notational differences with respect to $U(2, 2)$ like, for example, the "parity reversal" operation in some expressions like (22) [the reader can consult [43] for the non-compact $U(2, 2)$ case]. We just use relativistic notation for convenience.

As we already said in (11) for the monolayer case, with this differential realization, the (cumbersome) computation of expectation values of operators in a coherent state (usually related to order parameters in the mean-field approximation) is reduced to the (easy) calculation of derivatives of the Bergmann kernel (20) as:

$$\langle Z|T_{\mu\nu}|Z\rangle = K_\lambda^{-1}(Z, Z^\dagger)\mathcal{T}_{\mu\nu}K_\lambda(Z, Z^\dagger).$$

(29)

We shall use this simple formula to compute the energy surface (the CS expectation value $\langle Z|H|Z\rangle$ of the Hamiltonian H). For example, in terms of $M_{\mu\nu} = 2i\lambda\frac{z_\mu\bar{z}^\nu - z_\nu\bar{z}^\mu}{\det(\sigma_0 + Z^\dagger Z)}$, the CS expectation values of spin and ppin operators turns out to be

$$\langle S_1\rangle = M_{23}, \ \langle S_2\rangle = M_{31}, \ \langle S_3\rangle = M_{12},$$
$$\langle R_{k3}\rangle = iM_{0k}, \ \langle\vec{S}\rangle^2 + \langle\vec{R}_3\rangle^2 = M_{\mu\nu}M^{\mu\nu}/2,$$
$$\langle P_1\rangle = \lambda\,\mathrm{Re}[\mathrm{tr}(Z)(1 + \det(Z^\dagger)]/\det(\sigma_0 + ZZ^\dagger),$$
$$\langle P_3\rangle = \lambda(\det(Z^\dagger Z) - 1)/\det(\sigma_0 + Z^\dagger Z),$$

(30)

where Re denotes the real part [$\langle P_2\rangle$ corresponds to the imaginary part] and i is the imaginary unit. Note that the following identity for the magnitude of the $SU(4)$ isospin is automatically fulfilled for coherent state expectation values:

$$\langle\vec{S}\rangle^2 + \langle\vec{P}\rangle^2 + \langle\mathbf{R}\rangle^2 = \lambda^2.$$

(31)

For $\lambda = 1$ it coincides with the variational ground state condition provided in [6]. For BLQH systems at $\nu =$

$2/\lambda$ we have seen in [22] that the spin and ppin phases are characterized by maximum values of $\langle \vec{S} \rangle^2 = \lambda^2$ and $\langle \vec{P} \rangle^2 = \lambda^2$, respectively.

The Husimi function $Q_\psi(Z)$ of a given state $|\psi\rangle$ is the CS expectation value $Q_\psi(Z) = \langle Z|\rho|Z\rangle$ of the corresponding density matrix $\rho = |\psi\rangle\langle\psi|$ (this definition can be directly extended to mixed states). $Q_\psi(Z)$ provides the probability of finding $|\psi\rangle$ in a coherent state $|Z\rangle$. For example, for $|\psi\rangle = |_{q_a,q_b}^{j,m}\rangle$ the Husimi function follows a multivariate distribution function [20]. Taking into account the CS closure relation $1 = \int_{\mathbb{G}_2^4} |Z\rangle\langle Z|d\mu(Z,Z^\dagger)$ with integration measure (25), we see that Q_ψ is normalized according to $\int_{\mathbb{G}_2} Q_\psi(Z)d\mu(Z,Z^\dagger) = 1$ for unit norm states $\langle\psi|\psi\rangle = 1$. The Husimi second moment is defined as [compare with the monolayer case in (12)]

$$M_\psi = \int_{\mathbb{G}_2} Q_\psi^2(Z)d\mu(Z,Z^\dagger). \tag{32}$$

As for the monolayer case, we shall conjecture that M_ψ attains its maximum value (maximum localization) when $|\psi\rangle$ is itself a CS. This conjecture has been proved for harmonic oscillator CS [35] and spin-s or $SU(2)$ CS [36]. We have calculated this maximum value for each λ in [20] and it turns out to be:

$$M_{\max}(\lambda) = \frac{1}{16} - \frac{1/2}{1+\lambda} + \frac{45/32}{1+2\lambda} + \frac{3/32}{3+2\lambda}, \tag{33}$$

which tends to $M_{\max}(\infty) = 1/16$ for high isospin λ values. Here we shall see that the ground state of a BLQH system attains this maximum value in spin a ppin phases, thus indicating that it is maximally localized in these phases (see next section).

IV. MODEL HAMILTONIAN AND QUANTUM PHASES

In Ref. [22] we have analyzed the ground state structure of BLQH at $\nu = 2/\lambda$. The Hamiltonian we used is an adaptation of the Landau-site Hamiltonian for $\nu = 2$ considered in [6]

$$H = H_{\text{C}} + H_{\text{ZpZ}}. \tag{34}$$

which consists of Coulomb and a combination of Zeeman and pseudo-Zeeman interactions. Discarding $U(4)$-invariant terms, the Coulomb part

$$H_{\text{C}} = 4\varepsilon_{\text{D}}^- P_3^2 - 2\varepsilon_{\text{X}}^-(\vec{S}^2 + \vec{R}_3^2 + P_3^2), \tag{35}$$

is a sum of the naive capacitance (ε_{D}^-) and the exchange (ε_{X}^-) interactions. The exchange and capacitance energy gaps are given in terms of the interlayer distance δ by

$$\varepsilon_{\text{X}}^\pm = \frac{1}{4}\sqrt{\frac{\pi}{2}}\left(1 \pm e^{(\delta/\ell_B)^2/2}\text{erfc}\left(\frac{\delta}{\sqrt{2}\ell_B}\right)\right)\mathcal{E}_C, \tag{36}$$

and $\varepsilon_{\text{D}}^- = \frac{\delta}{4\ell_B}\mathcal{E}_C$, where $\mathcal{E}_C = e^2/(4\pi\epsilon\ell_B)$ is the Coulomb energy unit and $\ell_B = \sqrt{\hbar c/(eB)}$ the magnetic length. In the following we shall simply put $\varepsilon_{\text{X}}^- = \varepsilon_{\text{X}}$ and $\varepsilon_{\text{D}}^- = \varepsilon_{\text{D}}$ as no confusion will arise. We shall usually choose $\delta = \ell_B$, which gives $\varepsilon_{\text{X}} \simeq 0.15$ in Coulomb units (we shall use Coulomb units throughout the article unless otherwise stated). The (pseudo) Zeeman part

$$H_{\text{ZpZ}} = -\Delta_{\text{Z}}S_3 - \Delta_{\text{t}}P_1 - \Delta_{\text{b}}P_3 \tag{37}$$

is comprised of: Zeeman (Δ_{Z}), interlayer tunneling (Δ_{t}, also denoted by Δ_{SAS} in the literature [7]) and bias (Δ_{b}) gaps. The bias term creates an imbalanced configuration between layers.

For $\nu = 2/\lambda$ ($N = 2\lambda$ flux quanta), Coulomb (two-body) interactions must be renormalized by the number of boson pairs $N(N-1)$, whereas one-body interactions must be renormalized by N, in order to make the energy an intensive quantity. Therefore, the Hamiltonian proposed for arbitrary λ is an adaptation of (34) of the form

$$H_\lambda = \frac{H_{\text{C}}}{N(N-1)} + \frac{H_{\text{ZpZ}}}{N}, \quad N = 2\lambda. \tag{38}$$

To study the semiclassical limit, we now replace the operators P_j, S_j and R_{ij} by their expectation values (30) in a isospin-λ coherent state $|Z\rangle$.

A minimization process of the ground state energy surface $\langle Z|H_\lambda|Z\rangle$ reveals the existence of three quantum phases: spin, canted and ppin, which are characterized by maximum and minimum values of the squared spin $\langle \vec{S} \rangle^2$ and squared ppin $\langle \vec{P} \rangle^2$ CS expectation values (order parameters). For the sake of simplicity, let us restrict ourselves, for this semiclassical analysis, to the balanced case (i.e. we discard therms proportional to ε_{D} and Δ_{b}). Using the parametrization (26) of Z, we found in [22] the common relations

$$\beta_+ = \beta_- = 0, \; \vartheta_+ + \vartheta_- = \pi, \; \theta_a + \theta_b = \pi, \; \phi_a = \phi_b. \tag{39}$$

in all phases. This leaves only two free parameters, for instance, ϑ_+ and θ_b. In the spin and ppin phases we have

$$\text{Spin}: \vartheta_+^s = 0 = \theta_a^s, \; \text{Ppin}: \vartheta_+^p = -\pi/2 = \theta_a^p, \tag{40}$$

respectively. In the canted phase we get the more involved expression

$$\tan\vartheta_+^c = \pm\sqrt{\frac{(\Delta_{\text{t}}^2 - \Delta_{\text{Z}}^2)^2 - (4\Delta_{\text{Z}}\varepsilon_{\text{X}}(\lambda))^2}{-(\Delta_{\text{t}}^2 - \Delta_{\text{Z}}^2)^2 + (4\Delta_{\text{t}}\varepsilon_{\text{X}}(\lambda))^2}}, \tag{41}$$

$$\tan\theta_b^c = \mp\frac{\Delta_{\text{t}}}{\Delta_{\text{Z}}}\sqrt{\frac{(\Delta_{\text{t}}^2 - \Delta_{\text{Z}}^2)^2 - (4\Delta_{\text{Z}}\varepsilon_{\text{X}}(\lambda))^2}{-(\Delta_{\text{t}}^2 - \Delta_{\text{Z}}^2)^2 + (4\Delta_{\text{t}}\varepsilon_{\text{X}}(\lambda))^2}},$$

where we have defined $\varepsilon_{\text{X}}(\lambda) = \lambda\varepsilon_{\text{X}}/(2\lambda-1)$. The phase transition points (spin-canted and canted-ppin) depend on λ and are located at

$$\Delta_{\text{t}}^{\text{sc}}(\lambda) = \sqrt{\Delta_{\text{Z}}^2 + 4\varepsilon_{\text{X}}(\lambda)\Delta_{\text{Z}}}, \tag{42}$$

$$\Delta_{\text{t}}^{\text{cp}}(\lambda) = 2\varepsilon_{\text{X}}(\lambda) + \sqrt{\Delta_{\text{Z}}^2 + 4\varepsilon_{\text{X}}^2(\lambda)}.$$

For $\Delta_t < \Delta_t^{sc}(\lambda)$ the BLQH system at $\nu = 2/\lambda$ is in the spin phase, for $\Delta_t^{sc}(\lambda) \leq \Delta_t \leq \Delta_t^{cp}(\lambda)$ it is in the canted phase and for $\Delta_t > \Delta_t^{cp}(\lambda)$ it is in the ppin phase [see [22] for more details]. Note that we have two different solutions of $(\vartheta_+^c, \theta_b^c)$ in the canted phase, given by the signs $(+,-)$ and $(-,+)$ in equation (41), leading to the same minimum energy $\langle Z_\pm^c | H_\lambda | Z_\pm^c \rangle$, with $Z_\pm^c = Z(\theta_{a,b}, \phi_{a,b}, \vartheta_\pm, \beta_\pm)|_\pm^c$ the corresponding stationary point in the Grassmannian $\mathbb{G}_2^4$ for any of the two solutions $(+) = (+,-)$ and $(-) = (-,+)$ together with the common restrictions (39). Even though both coherent states $|Z_+^c\rangle$ and $|Z_-^c\rangle$ give the same CS energy expectation value $\langle Z_+^c | H_\lambda | Z_+^c \rangle = \langle Z_-^c | H_\lambda | Z_-^c \rangle$ (see [22]), they are distinct; in fact, they are almost orthogonal $\langle Z_+^c | Z_-^c \rangle \simeq 0$ in the canted phase. This indicates that the ground state is degenerated and there is a broken symmetry in the thermodynamic limit. Let us study the ground state structure in the phase-space (Bargmann) picture of section III.

V. GROUND STATE ANALYSIS IN PHASE-SPACE AND LOCALIZATION MEASURES

A. Variational results

We start with the analysis of the variational ground state. Let us denote collectively by Z_+^0 and Z_-^0 the two sets of stationary points in any of the three (spin, canted and ppin) quantum phases (note that $Z_+^0 = Z_-^0$ in the spin and ppin phases). A good variational approximation to the true ground state is achieved by taking the normalized symmetric combination

$$|Z_{\text{sym}}^0\rangle = \frac{|Z_+^0\rangle + |Z_-^0\rangle}{\sqrt{2(1 + \text{Re}(\langle Z_+^0 | Z_-^0 \rangle))}}. \quad (43)$$

This is a quantum superposition of two coherent (semiclassical) states. Using the general expression of the CS overlap (24) and the Bergmann kernel $K_\lambda(Z'^\dagger, Z) = [1 + \text{tr}(Z'^\dagger Z) + \det(Z'^\dagger Z)]^\lambda$, we can easily compute the corresponding Husimi function

$$Q_{\text{sym}}^0(Z) = |\langle Z_{\text{sym}}^0 | Z \rangle|^2 = \frac{|\langle Z_+^0 | Z \rangle + \langle Z_-^0 | Z \rangle|^2}{2(1 + \text{Re}(\langle Z_+^0 | Z_-^0 \rangle))}. \quad (44)$$

We shall restrict, for the sake of simplicity, to the plane (ϑ_+, θ_b) of the 8-dimensional Grassmannian phase-space $\mathbb{G}_2^4$ with constraints (39), where non-trivial angle values (41) are found in the canted phase. In the plane (ϑ_+, θ_b), the Husimi function adopts a quite simple form given by

$$Q_{\text{sym}}^0(\vartheta_+, \theta_b) = \frac{(\cos(\vartheta_+ - \vartheta_+^0) + \cos(\theta_b - \theta_b^0))^{2\lambda}}{2^{2\lambda}}, \quad (45)$$

where $(\vartheta_+^0, \theta_b^0)$ must be replaced by (40) and (41) in the spin, ppin and canted phases, respectively. In

Figure 1 we represent a contour plot of $Q_{\text{sym}}^0(\vartheta_+, \theta_b)$ in the three phases. We see that the variational state is localized around $(\vartheta_+^s, \theta_b^s) = (0,0)$ [or equivalently $(\vartheta_+^s, \theta_b^s) = (\pi, \pi)$] in the spin phase, and around $(\vartheta_+^p, \theta_b^s) = (\pi/2, \pi/2)$ in the ppin phase. In both, spin and ppin, phases we have $|Z_+^0\rangle = |Z_-^0\rangle$ and therefore $|Z_{\text{sym}}^0\rangle$ is coherent. In the canted phase, the variational ground state splits into two different packets, $|Z_+^c\rangle \neq |Z_-^c\rangle$, localized around the two stationary solutions (41). Both packets have negligible overlap $\langle Z_+^c | Z_-^c \rangle \simeq 0$ and recombine in the spin and ppin regions. This kind of quantum superpositions of two semiclassical states with negligible overlap is sometimes referred to as a "Schrödinger cat" state in the literature, and they have many interesting physical properties in quantum information processing.
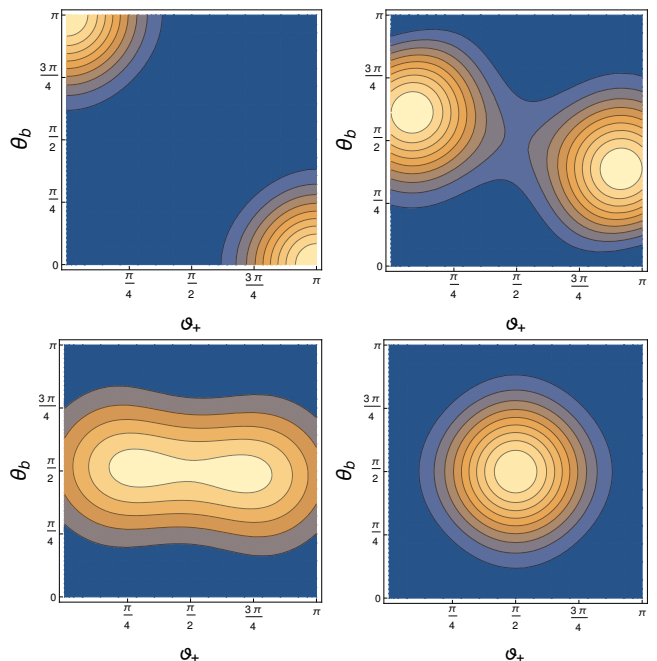

FIG. 1: Contour plot of the Husimi function (44) of the variational ground state in the plane (ϑ_+, θ_b) of the phase-space $\mathbb{G}_2^4$ for $\lambda = 3$, Zeeman $\Delta_Z = 0.01$, layer distance $\delta = \ell_B$ and four values of tunneling gap Δ_t. The top-left panel corresponds to the spin phase ($\Delta_t = 0.01$), the top-right and bottom-left panels correspond to the canted phase ($\Delta_t = 0.1$ and $\Delta_t = 0.2$, respectively) and the bottom-right panel corresponds to the canted phase ($\Delta_t = 0.5$). Lighter zones correspond to higher values of the Husimi function, that is, to higher probability for the ground state to be coherent.

This delocalization of $|Z_{\text{sym}}^0\rangle$ in phase-space inside the canted phase is captured by the Husimi function second moment (32). Indeed, in figure 2 we represent the localization of the variational and exact (see next section) ground state in phase-space measured by the Husimi second moment as a function of the tunneling Δ_t (we fix $\Delta_Z = 0.01$ and $\delta = \ell_B$). We compare the two cases: $\lambda = 1$ and $\lambda = 3$. In the spin and ppin phases

we have maximum localization [maximum moment (33)], giving $M_{\max}(1) = 3/10$ and $M_{\max}(3) = 25/168$, since the ground state is a (minimal uncertainty) coherent state [note that, in the exact case, the maximum moment value is only attained asymptotically in the ppin phase]. In the transition from the spin to the canted phase we observe a sudden delocalization (a drop of the Husimi second moment) of the ground state wave function in phase-space. Therefore, the canted region is characterized for having a much more delocalized ground state than in the spin and ppin regions. Thus, we conclude that the Husimi second moment serves as an order parameter characterizing the three phases and the phase transition points.
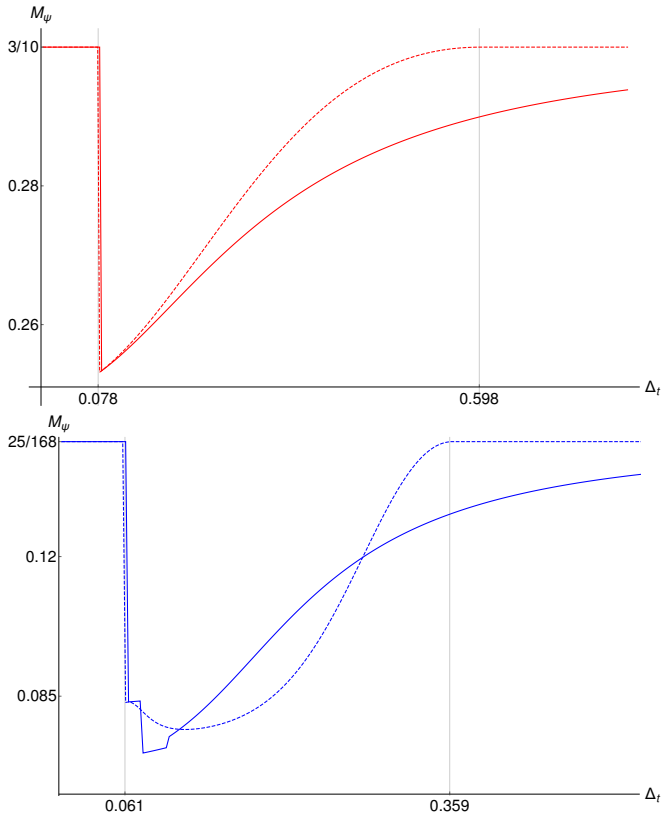
FIG. 2: Second moment M_ψ of the Husimi function Q_ψ of the variational (dashed) and exact (solid) ground states ψ as a function of the tunneling Δ_t for Zeeman $\Delta_Z = 0.01$, interlayer distance $\delta = \ell_B$ and $\lambda = 1$ (top red) and $\lambda = 3$ (bottom blue). Maximum moments values (33) for $\lambda = 1$ and $\lambda = 3$ are $3/10$ and $25/168$, respectively. Spin-canted, $\Delta_t^{\mathrm{sc}}(1) = 0.078$ and $\Delta_t^{\mathrm{sc}}(3) = 0.061$, and canted-ppin, $\Delta_t^{\mathrm{cp}}(1) = 0.598$ and $\Delta_t^{\mathrm{cp}}(3) = 0.359$, phase-transition points (42) are marked by vertical dotted grid lines.

In figure 3 we make a 3-dimensional representation and a contour-plot of $M_{|Z^0_{\mathrm{sym}}\rangle}$ as a function of tunneling Δ_t and Zeeman Δ_Z gaps for $\lambda = 1$ and $\lambda = 3$ (we take $\delta = \ell_B$). The figure 2 corresponds to a cross-section at $\Delta_Z = 0.01$. We see as the valley of $M_{|Z^0_{\mathrm{sym}}\rangle}$ (delocalized state), represented by darker zones of the contour-plot,

captures the canted phase in the Δ_t-Δ_Z control parameter plane. The transition from canted to ppin phase is better marked (sharp) for $\lambda = 3$ than for $\lambda = 1$.
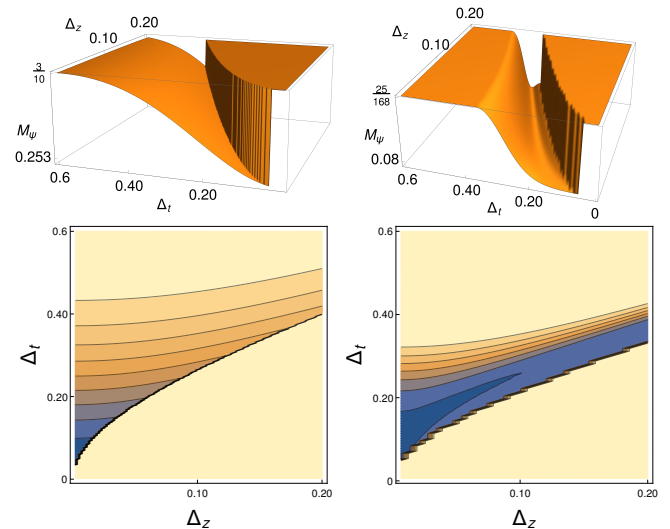

FIG. 3: Second moment of the Husimi function of the variational ground state as a function of tunneling Δ_t and Zeeman Δ_Z gaps for $\lambda = 1$ (left) and $\lambda = 3$ (right). Interlayer distance $\delta = \ell_B$. We make a 3D plot (top) and a contour-plot (bottom). The canted phase is characterized by the moment valleys (darker zones of the contour-plot), where the wave function is more delocalized. Spin and ppin phases are characterized by high moment values (lighter zones of the contour-plot), where the wave function is more localized (coherent). The transition from canted to ppin is better marked for $\lambda = 3$ that for $\lambda = 1$.

B. Numeric diagonalization results

Now we shall diagonalize the Hamiltonian (38) and obtain the corresponding ground state. We shall call it "exact" in contrast to the variational ground state discussed in the previous section. For zero tunneling $\Delta_t = 0$, the Hamiltonian is diagonal in the orthonormal basis (16). Its eigenvalues can be straightforwardly obtained from (21) as

$$E_\lambda\binom{j,m}{q_a,q_b} = \frac{\varepsilon_{\mathrm{cap}}(2j + 2m - \lambda)^2 - 8\varepsilon_X j(j+1)}{2\lambda(2\lambda - 1)} - \frac{\Delta_Z(q_b - q_a) + \Delta_b(2j + 2m - \lambda)}{2\lambda}, (46)$$

where $\varepsilon_{\mathrm{cap}} = 4\varepsilon_D - 2\varepsilon_X$ denotes the capacitance energy.

Looking at $E_\lambda\binom{j,m}{q_a,q_b}$, for small bias Δ_b, the lowest energy state must have zero capacitance energy (note that $\varepsilon_{\mathrm{cap}} \geq 0$), that is, it must be balanced $2j + 2m - \lambda = 0$. It must also have maximum angular momentum $j = \lambda/2 \Rightarrow m = 0$ [remember the constraint $2j + m \leq \lambda$ in (18)], which gives the minimum exchange energy. Also, the

Zeeman energy attains its minimum for $q_b = \lambda/2 = -qa$. Therefore, the ground state at $\Delta_t = 0$ and small Δ_b is the basis state $|\psi_0^s\rangle = |^{\lambda/2,\ 0}_{-\lambda/2,\lambda/2}\rangle$, which coincides with the variational CS $|Z_{\text{sym}}^0\rangle = |Z_+^0\rangle$ in the spin phase. Actually, the ground state in the spin phase is always $|^{\lambda/2,\ 0}_{-\lambda/2,\lambda/2}\rangle$, independent of the control parameters $(\Delta_t, \Delta_Z, \Delta_b)$, and the squared spin expectation value is $\langle\psi_0^s|\vec{S}|\psi_0^s\rangle^2 = \lambda^2$, thus attaining its maximum value [remember the identity (31)].

For high bias voltage, the dominant part of the energy goes as $-\Delta_b(2j + 2m - \lambda)$ which attains its minimum for $j = 0$ and $m = \lambda$ (maximum positive imbalance, i.e. all flux quanta in layer a). This corresponds to the ppin phase and the ground state in this case is $|\psi_0^p\rangle = |^{0,\lambda}_{0,0}\rangle$. This also turns out to be a CS, in fact a particular case of (22) given by

$$|\psi_0^p\rangle = |Z_\infty\rangle = \frac{\det(\mathbf{a}^\dagger)^\lambda|0\rangle_F}{\lambda!\sqrt{\lambda+1}}. \qquad (47)$$

The squared ppin expectation value is $\langle\psi_0^p|\vec{P}|\psi_0^p\rangle^2 = \lambda^2$, thus attaining its maximum value.

For non-zero tunneling, the Hamiltonian (38) is not diagonal in the orthonormal basis (16). Indeed, the matrix elements of the interlayer tunneling operator are

$$P_1|^{j,m}_{q_a,q_b}\rangle = C^{j,m+1}_{q_a,q_b}|^{j-\frac{1}{2},m+1}_{q_a-\frac{1}{2},q_b-\frac{1}{2}}\rangle + C^{j,m+1}_{-q_a,-q_b}|^{j-\frac{1}{2},m+1}_{q_a+\frac{1}{2},q_b+\frac{1}{2}}\rangle +$$

$$C^{j+\frac{1}{2},m+2j+2}_{-q_a+\frac{1}{2},-q_b+\frac{1}{2}}|^{j+\frac{1}{2},m}_{q_a-\frac{1}{2},q_b-\frac{1}{2}}\rangle + C^{j+\frac{1}{2},m+2j+2}_{q_a+\frac{1}{2},q_b+\frac{1}{2}}|^{j+\frac{1}{2},m}_{q_a+\frac{1}{2},q_b+\frac{1}{2}}\rangle +$$

$$C^{j,m+2j+1}_{q_a,q_b}|^{j-\frac{1}{2},m}_{q_a-\frac{1}{2},q_b-\frac{1}{2}}\rangle + C^{j+\frac{1}{2},m}_{-q_a+\frac{1}{2},-q_b+\frac{1}{2}}|^{j+\frac{1}{2},m-1}_{q_a-\frac{1}{2},q_b-\frac{1}{2}}\rangle +$$

$$C^{j,m+2j+1}_{-q_a,-q_b}|^{j-\frac{1}{2},m}_{q_a+\frac{1}{2},q_b+\frac{1}{2}}\rangle + C^{j+\frac{1}{2},m}_{q_a+\frac{1}{2},q_b+\frac{1}{2}}|^{j+\frac{1}{2},m-1}_{q_a+\frac{1}{2},q_b+\frac{1}{2}}\rangle, \qquad (48)$$

where the coefficients C where calculated in [18] and are given by

$$C^{j,m}_{q_a,q_b} = \frac{1}{2}\frac{\sqrt{(j+q_a)(j+q_b)m(\lambda-(m-2))}}{\sqrt{2j(2j+1)}}, \ j \neq 0, \qquad (49)$$

and $C^{j,m}_{q_a,q_b} = 0$ for $j = 0$. Taking into account the matrix elements (21) and (48), we can calculate the Hamiltonian matrix elements $\langle J|H_\lambda|J'\rangle$, where $J = \{^{j,m}_{q_a,q_b}\}$ denotes a multi-index running from $J = 1, \ldots, d_\lambda$. The ground state $|\psi_0\rangle$ is a linear combination of the basis states $|J\rangle$ as

$$|\psi_0(\Delta)\rangle = \sum_{J=1}^{d_\lambda} c_J(\Delta)|J\rangle, \qquad (50)$$

with coefficients $c_J(\Delta)$ depending on the Zeeman, tunneling, bias, etc, control parameters (generically denoted by Δ). The Husimi function is then

$$Q_{\psi_0(\Delta)}(Z) = |\langle Z|\psi_0(\Delta)\rangle|^2 \qquad (51)$$

$$= \sum_{J,J'=1}^{d_\lambda} \frac{\overline{\varphi_J(Z)}\varphi_{J'}(Z)}{\det(\sigma_0+Z^\dagger Z)^\lambda} c_J(\Delta)\overline{c_{J'}(\Delta)},$$

where $\varphi_J(Z)$ are the homogeneous polynomials (18). The corresponding Husimi function second moment (32) is then given by

$$M_{\psi_0}(\Delta) = \sum_{J,J',K,K'=1}^{d_\lambda} c_J(\Delta)\overline{c_{J'}(\Delta)}c_K(\Delta)\overline{c_{K'}(\Delta)}$$

$$\times \int_{\mathbb{G}_2^4} \frac{\overline{\varphi_J(Z)}\varphi_{J'}(Z)\overline{\varphi_K(Z)}\varphi_{K'}(Z)}{\det(\sigma_0+Z^\dagger Z)^{2\lambda}} d\mu(Z, Z^\dagger). \qquad (52)$$

We have performed a numerical diagonalization of the Hamiltonian (38) for $\lambda = 1$ (dimension $d_1 = 6$) and $\lambda = 3$ (dimension $d_3 = 50$) using a mesh of 300 points, with a resolution of tunneling gap $\Delta_t = 0.5$ in figure 2, and a mesh of 100×30 points, with a resolution of $\Delta_t = 0.6$ and $\Delta_Z = 0.2$ in the 3D figure 5. The multiple integrals in the 8-dimensional Grassmannian $\mathbb{G}_2^4$ are also calculated numerically. They are computationally quite hard calculations. In figure 2 we compare variational (dashed curves) with exact (solid curves) values of the Husimi function second moment of the ground state. We see that the variational approximation agrees with the exact calculation in the spin phase and captures quite well the delocalization of the ground state in phase space inside the canted region. In the ppin region, both the variational and exact grouns states become again localized although, in the exact case, the maximum moment value is only attained asymptotically for high Δ_t. This agreement between variational and exact ground states is also patent when comparing figure 1 with 4 and figure 3 with 5. The variational result captures quite faithfully the ground state structure and localization measures in the three phases.
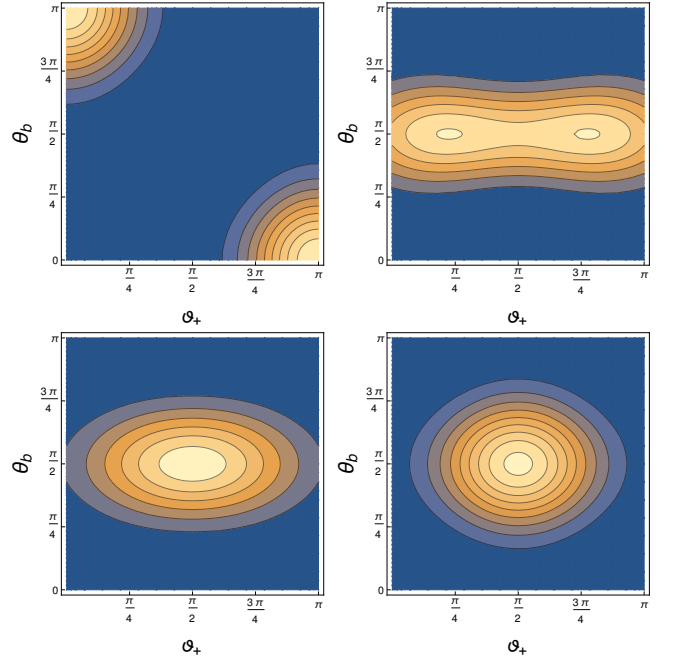

FIG. 4: Contour plot of the Husimi function Q_{ψ_0} of the exact ground state $|\psi_0\rangle$ in the plane (ϑ_+, θ_b) of the phase-space $\mathbb{G}_2^4$ for $\lambda = 3$. Same structure and values as in the variational case of figure 1.
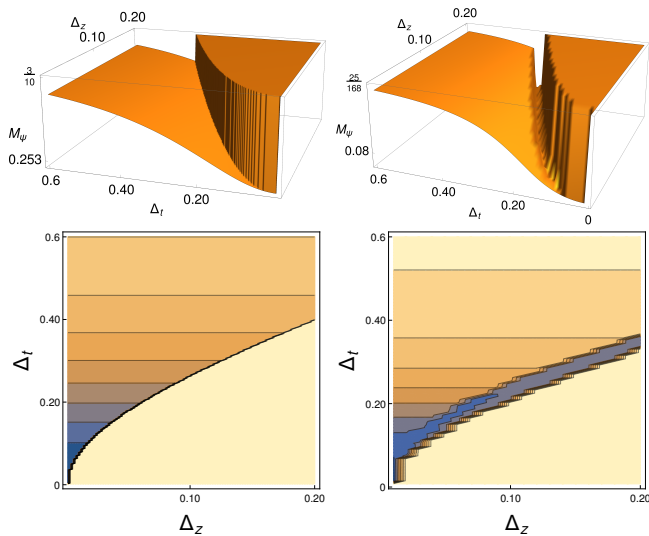
FIG. 5: Second moment of the Husimi function of the exact ground state as a function of tunneling Δ_t and Zeeman Δ_Z for $\lambda = 1$ (left) and $\lambda = 3$ (right). Same structure and values as in the variational case of figure 3.

FIG. 6: Second moment of the Husimi function of the exact ground state as a function of tunneling Δ_t and Zeeman Δ_Z for $\lambda = 3, \delta = \ell_B$ and bias voltage $\Delta_b = 0.5$ (left) and $\Delta_b = 1$ (right). For higher Δ_b, the ppin phase dominates more and more in the phase diagram Δ_Z-Δ_t.

In the analytical and variational studies developed in section IV, we have restricted ourselves to the balanced case, for the sake of simplicity. To finish, and for the sake of completeness, we study the effect of a non-zero bias voltage (non-balanced case) on the exact ground state ψ Husimi second moment M_ψ. In figure 6 we represent contour-plots of M_ψ as a function of tunneling Δ_t and Zeeman Δ_Z for $\lambda = 3$ and two values of bias voltage: $\Delta_b = 0.5$ and $\Delta_b = 1$. We see that a non-zero Δ_b modifies the spin-canted and canted-ppin phase transition points as regards the balanced case (42), here given by transitions from high to low momentum M_ψ. Therefore, the canted region, characterized by low momentum M_ψ (darker zones in the contour-plot), moves in the phase diagram Δ_t-Δ_Z when varying Δ_b. In particular, the second moment analysis also reproduces the already noticed fact that the ppin phase dominates at higher values of Δ_b.

VI. CONCLUSIONS AND OUTLOOK

Using a coherent state representation of the ground state ψ, in the Grassmannian phase space $\mathbb{G}_2^4$, given by the Husimi Q_ψ function, we have characterized the three quantum phases (spin, ppin and canted) of BLQH system models at fractional filling factors $\nu = 2/\lambda$. We have found that the Husimi function second moment quantifies the localization (inverse volume) of ψ in phase space and serves as an order parameter distinguishing the spin and ppin phases (high localization) from the canted phase (low localization). Otherwise stated, the ground state in spin and ppin phases is highly coherent, whereas in the canted phase it is a kind of Schrödinger cat, i.e., a superposition of two coherent (quasi-classical, minimal uncer-
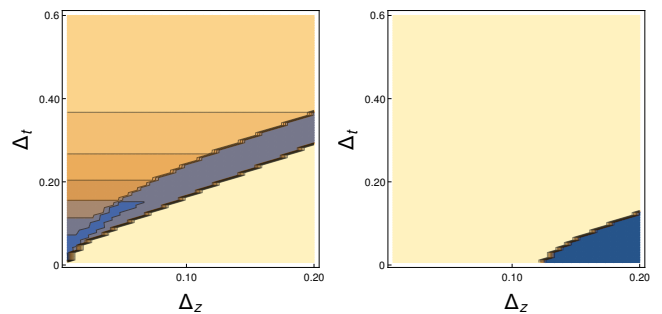
tainty) states with negligible overlap. We have also visualized the ground state Husimi function in the spin, ppin and canted phases using two-dimensional cross-sections of the 8-dimensional Grassmannian phase space $\mathbb{G}_2^4$. The variational (analytic) treatment produces good qualitative and quantitative results as regards the exact (numeric) diagonalization calculations.

We believe that this CS picture of BLQH systems provides an alternative and useful tool and a new perspective compared to more traditional approaches to the subject. Indeed, the potentialities of the Husimi approach go far beyond the localization analysis of quantum phases studied in this article. For example, there is possibility of quantum state reconstruction mentioned at the introduction. The implementation of these techniques (mainly imported from quantum optics) in multilayer quantum Hall devices, could open new possibilities for the design and use of these nanostructures in quantum informations protocols. Actually, one can find quantum computation proposals using BLQH systems in, for example, [44, 45]. The objective is to engineer quantum Hall states to eventually implement large scale quantum computing in multilayer QH systems. For this purpose, controllable (spin and ppin) entanglement [19, 46, 47], robustness of qubits (long decoherence time and robust interlayer phase difference) [45] and easy qubit measurement are crucial. For example, in reference [44] it is theoretically shown that spontaneously interlayer-coherent BLQH droplets should allow robust and fault-tolerant pseudospin quantum computation in semiconductor nanostructures. We believe that our BLQH CS $|Z\rangle$ at $\nu = 2/\lambda$ will play an important role, not only in theoretical considerations but, also in experimental settings.

Moreover, the analysis of small fluctuations around the ground state is usually described by a $U(N)$-invariant nonlinear sigma model Lagrangian which, for $N = 4$ and filling factor $\nu = 2$ acquires the form

$$L = \text{tr}\left[(\sigma_0 + ZZ^\dagger)^{-1}\partial^\alpha Z(\sigma_0 + Z^\dagger Z)^{-1}\partial_\alpha Z^\dagger\right], \quad (53)$$

(plus a Berry phase term) where $Z = z^\mu \sigma_\mu$ is the dynam-

ical $\mathbb{G}_2^4$ field $Z(x)$ (Goldstone modes) in $(2+1)$ dimensions ($\alpha = 0, 1, 2$). This is a generalization of the original Haldane's [48] description of the continuum field theory describing the low-energy dynamics of the large-spin two-component Heisenberg anti-ferromagnet in terms of a $O(3)$-invariant nonlinear sigma model. In fact, this picture can be extended to more general N-component fractional quantum Hall systems at $\nu = M/\lambda$ and nonlinear sigma models on $\mathbb{G}_M^N$ have already been proposed in [21]. The structure of the Husimi amplitude $\psi(Z)$ of the ground state ψ, in each phase, obtained in this article, will be essential to analyze the Goldstone modes describing the small fluctuations around the ground state inside

these nonlinear sigma models on Grassmannians. This is work in progress.

Acknowledgements

[1] P.W. Anderson, Absence of Diffusion in Certain Random Lattices, Phys. Rev. 109, 1492 (1958).

[2] F. Wegner, Inverse Participation Ratio in $2 + \epsilon$ Dimensions, Z. Phys. B 36, 209 (1980)

[3] T. Brandes, S. Kettemann, Anderson Localization and Its Ramifications: Disorder, Phase Coherence and Electron Correlations, Lecture Notes in Physics 630, Springer 2003

[4] C. Aulbach, A. Wobst, G.-L. Ingold, P. Hanggi, and I. Varga, Phase-space visualization of a metal-insulator transition, New J. Phys. 6, 70 (2004).

[5] F. Evers and A. D. Mirlin, Anderson transitions, Rev. Mod. Phys. 80, 1355 (2008)

[6] Z.F. Ezawa, M. Eliashvili, G. Tsitsishvili, Ground-state structure in $\nu = 2$ bilayer quantum Hall systems. Phys. Rev. B71 (2005) 125318

[7] Z. F. Ezawa, Quantum Hall Effects: Field Theoretical Approach and Related Topics, 2nd Edition (World Scientific, Singapore 2008)

[8] A. H. MacDonald, R. Rajaraman and T. Jungwirth, Broken-symmetry ground states in $\nu = 2$ bilayer quantum Hall systems, Phys. Rev. B 60, 8817 (1999)

[9] L. Brey, E. Demler and S. Das Sarma, Electromodulation of the Bilayered $\nu = 2$ Quantum Hall Phase Diagram, Phys. Rev. Lett. 83 (1999) 168-171

[10] J. Schliemann A. H. MacDonald, Bilayer Quantum Hall Systems at Filling Factor $\nu = 2$: An Exact Diagonalization Study, Phys. Rev. Lett. 84 (2000) 4437.

[11] K. Hasebe and Z. F. Ezawa, Grassmannian fields and doubly enhanced Skyrmions in the bilayer quantum Hall system at $\nu = 2$, Phys. Rev. B66, 155318 (2002)

[12] A. Fukuda, A. Sawada, S. Kozumi, D. Terasawa, Y. Shimoda, Z. F. Ezawa, N. Kumada, and Y. Hirayama, Magnetotransport study of the canted antiferromagnetic phase in bilayer $\nu = 2$ quantum Hall state, Phys. Rev. B73 (2006) 165304

[13] F.D.M. Haldane, Fractional Quantization of the Hall Effect: A Hierarchy of Incompressible Quantum Fluid States, Phys. Rev. Lett. 51 (1983) 605-608

[14] J.R. Klauder and Bo-Sture Skagerstam, Coherent States: Applications in Physics and Mathematical Physics, World Scientific (1985)

[15] A. Perelomov, Generalized Coherent States and Their Aplications, Springer-Verlag (1986)

[16] J-P. Gazeau, Coherent States in Quantum Physics,

Wiley-VCH, Berlin, 2009.

[17] S.T. Ali, J.-P. Antoine, J.-P. Gazeau, Coherent States, Wavelets and Their Generalizations, Springer, second edition (2014).

[18] M. Calixto and E. Pérez-Romero, Coherent states on the Grassmannian $U(4)/U(2)^2$: Oscillator realization and bilayer fractional quantum Hall systems, J. Phys. A: Math. Theor. 47, (2014) 115302.
Erratum: there is a misprint in equation (49) of this reference. One must replace $C_{\cdot,\cdot}^{\cdot,2j+m+1}$ by $C_{\cdot,\cdot}^{\cdot,2j+m+2}$.

[19] M. Calixto and E. Pérez-Romero, Interlayer coherence and entanglement in bilayer quantum Hall states at filling factor $\nu = 2/\lambda$, J. Phys.: Condens. Matter 26 (2014) 485005

[20] M. Calixto and E. Pérez-Romero, Some properties of Grassmannian $U(4)/U(2)^2$ coherent states and an entropic conjecture, J. Phys. A: Math. Theor. 48 (2015) 495304

[21] M. Calixto, C. Peón-Nieto and E. Pérez-Romero, Coherent states for N-component fractional quantum Hall systems and their nonlinear sigma models, Annals of Physics 373 (2016) 52-66

[22] M. Calixto, C. Peon-Nieto and E. Perez-Romero, Hilbert space and ground state structure of bilayer quantum Hall systems at $\nu = 2/\lambda$, Phys. Rev. B95 (2017) 235302.
DOI: 10.1103/PhysRevB.95.235302, arXiv:1703.05021v2

[23] U. Leonhardt, Measuring the Quantum State of Light, New York: Cambridge University Press (1997)

[24] Gerhard Kirchmair, Brian Vlastakis, Zaki Leghtas, Simon E. Nigg, Hanhee Paik, Eran Ginossar, Mazyar Mirrahimi, Luigi Frunzio, S. M. Girvin and R. J. Schoelkopf, Observation of quantum state collapse and revival due to the single-photon Kerr effect, Nature 495, 205-209 (2013). doi:10.1038/nature11902

[25] F. J. Arranz, Z. S. Safi, R. M. Benito, and F. Borondo, Zeros of the Husimi function and quantum numbers in the HCP molecule, Eur. Phys. J. D 60, 279 (2010).

[26] F. J. Arranz, L. Seidel, C. G. Giralda, R. M. Benito, and F. Borondo, Onset of quantum chaos in molecular systems and the zeros of the Husimi function, Phys. Rev. E 87, 062901 (2013).

[27] D. Weinmann, S. Kohler, G.-L. Ingold, and P. Hänggi, Disordered systems in phase space, Ann. Phys. (Leipzig) 8, SI277 (1999).

[28] M. Calixto and E. Romera, Identifying topological-band

insulator transitions in silicene and other 2D gapped Dirac materials by means of Rényi-Wehrl entropy, EPL, 109 (2015) 40003

[29] E. Romera, R. del Real, and M. Calixto, Husimi distribution and phase-space analysis of a Dicke-model quantum phase transition, Phys. Rev. A 85, 053831 (2012).

[30] M. Calixto, R. del Real and E. Romera, Husimi distribution and phase-space analysis of a vibron-model quantum phase transition, Phys. Rev. A 86, 032508 (2012).

[31] O. Castaños, M. Calixto, F. Pérez-Bernal and E. Romera, Identifying the order of a quantum phase transition by means of Wehrl entropy in phase space, Phys. Rev. E 92, 052106 (2015)

[32] E. Romera, O. Castaños, M. Calixto and F. Pérez-Bernal, Delocalization properties at isolated avoided crossings in Lipkin-Meshkov-Glick type Hamiltonian models , J. Stat. Mech. 013101 (2017)

[33] C. Pérez-Campos, J.R. González-Alonso, O. Castaños, R. López-Peña, Entanglement and Localization of a Two-Mode Bose-Einstein Condensate, Annals of Physics 325, 325-344 (2010)

[34] M. Calixto, O. Castaños and E. Romera, Searching for pairing energies in phase space, EPL 108 (2014) 47001. doi: 10.1209/0295-5075/108/47001

[35] A. Wehrl, On the relation between classical and quantum mechanical entropies, Rep. Math. Phys. 16 353 (1979)

[36] E. H. Lieb and J. P. Solovej, Proof of an entropy conjecture for Bloch coherent spin states and its generalizations, Acta Math. 212, 379 (2014).

[37] J.K. Jain, Composite fermions, Cambridge University Press, New York, 2007.

[38] Saba M., Pasquini T. A., Sanner C., Shin Y., Ketterle W. and Pritchard D. E., Light Scattering to Determine the Relative Phase of Two Bose-Einstein Condensates, Science 307 (2005) 1945.

[39] I. Affleck, The quantum Hall effects, σ-models at $\theta = \pi$ and quantum spin chains, Nucl. Phys. B257 (1985) 397; I. Affleck, Exact critical exponents for quantum spin chains, non-linear σ-models at $\theta = \pi$ and the quantum hall effect, B265 (1986) 409-447; I. Affleck, Critical behaviour of SU(n) quantum chains and topological non-linear σ-models, Nucl. Phys. B305 (1988), 582-596

[40] N. Read and S. Sachdev, Some features of the phase diagram of the square lattice SU(N) antiferromagnet, Nucl. Phys. B316 (1989) 609

[41] D. P. Arovas, A. Karlhede and D. Lilliehöök, SU(N) quantum Hall skyrmions, Phys. Rev. B59 (1999) 13147-13150.

[42] L.C. Biedenharn, J.D. Louck, Angular Momentum in Quantum Physics, Addison-Wesley, Reading, MA, 1981; L.C. Biedenharn, J.D. Louck, The Racah-Wigner Algebra in Quantum Theory, Addison-Wesley, New York, MA 1981

[43] M. Calixto and E. Pérez-Romero, On the oscillator realization of conformal U(2,2) quantum particles and their particle-hole coherent states, J. Math. Phys. 55 (2014) 081706

[44] V. W. Scarola, K. Park, S. Das Sarma, Pseudospin Quantum Computation in Semiconductor Nanostructures, Phys. Rev. Lett. **91**, 167903 (2003)

[45] S.R.Eric Yang, J. Schliemann, and A. H. MacDonald, Quantum-Hall quantum bits, Phys. Rev. B **66**, 153302 (2002).

[46] B. Doucot, M. O. Goerbig, P. Lederer, R. Moessner, Entanglement skyrmions in multicomponent quantum Hall systems, Phys. Rev. B **78**, 195327 (2008)

[47] J. Schliemann, Entanglement spectrum and entanglement thermodynamics of quantum Hall bilayers at $\nu = 1$, Phys. Rev. B **83**, 115322 (2011)

[48] F.D.M. Haldane, Continuum dynamics of the 1-D Heisenberg antiferromagnet: Identification with the O(3) nonlinear sigma model, Phys. Lett. **A93** (1983) 464; F.D.M. Haldane, Nonlinear Field Theory of Large-Spin Heisenberg Antiferromagnets: Semiclassically Quantized Solitons of the One-Dimensional Easy-Axis Néel State, Phys. Rev. Lett. **50** (1983) 1153; F.D.M. Haldane, O(3) Nonlinear σ Model and the Topological Distinction between Integer- and Half-Integer-Spin Antiferromagnets in Two Dimensions, Phys. Rev. Lett. **61** (1988) 1029